J. Basic. Appl. Chem., 9(2)11-18, 2019

ISSN 2090-424X
Journal of Basic and Applied Chemistry
www.textroad.com

Potentiodynamic Study on the Effect of Expired Septazole and Septrin Drugs on the Corrosion Inhibition of Tin Electrode in 1M HCl Solution

E. M. Attia, N. S. Hassan and A. M. Hyba

Chemistry Department, Faculty of Science (Girls), Al-Azhar University, Nasr city, Cairo, Egypt

ABSTRACT

With the purpose of reducing the high cost of synthetic inhibitors, the expired Septazole (ESD) and Septrin (ESpD) drugs were tested as corrosion inhibitors for tin electrode in 1M HCl solution. Infra-red (IR) analysis was used to investigate the functional groups present in the expired drugs, while the morphology of the surface was studied by scanning electron microscope (SEM) analysis. Potentiodynamic polarization was applied to this study and illustrated that, ESD and ESpD acted as mixed type inhibitors at 20 and 30°C, and acted as cathodic inhibitors at 40, 50 and 60°C, with better inhibition effect of ESD than ESpD. The obtained results revealed that the higher temperature of solutions, the higher corrosion rates and subsequently the lower inhibition efficiency. This was done by physical adsorption on the tin surface.

KEYWORD: Expired drugs, Tin, Corrosion, Inhibition, Weight loss.

1. INTRODUCTION

Tin metal is widely used in many important industrial applications owing to its low melting point and tensile strength, high flexibility and good corrosion resistance. So tin represents a good area for researchers work [1-5]. Processes performed in industry extensively use mineral acids such as HCl and H_2SO_4. These acids cause severe corrosion to different usable industrial metals. One of the most popular methods of preventing this corrosive attack is the usage of inhibitors [6-10]. Drugs are classified as cheap, non-toxic and environmentally friendly. In recent years, the uses of expired drugs as corrosion inhibitors for different metals take the attention of many authors [11- 16]. Septazole is an antibacterial drug inhibited the corrosion of copper in 0.1M HCl. The potentiodynamic polarization tests performed in different concentrations illustrated that Septazole acted as mixed-type inhibitor [17]. Sulfamethoxazole is the active ingredient of Septazole. It is a famous type of sulfa drug, and it is a derivative of sulfanilamide. It is used with trimethoprim in a 5:1 ratio to produce other drugs as Septrin syrup. Sulfamethoxazole inhibits the corrosion of the brass in the synthetic acidic rainwater and the inhibition efficiency increased with increasing concentration and immersion time [18]. This provides a cost effective process to solve the corrosion issue. In this framework, we have examined the use of expired Septazole and Septrin drugs as corrosion inhibitors for tin in 1 M HCl.

2. EXPERIMENT

2.1. Electrode and solutions:-

The working electrode was made of a rod of tin with the chemical composition (wt %): 97.5 Sn; 0.78 Ti; 0.4 Si and 0.013 Fe, with contact surface area 2.27cm^2. Before each experiment the electrode surface was mechanically polished using successive grades of emery paper followed by washing with bidistilled water.

The corrosive solution was prepared by dilution of AR reagent grade 37% concentrated HCl using bi-distilled water to1M solution.

Septazole and Septrin syrups are antibiotic sulfa drugs. Each 5 ml of Septazole syrup contains 200 mg of the active sulfamethoxazole. Its empirical formula is $C_{10}H_{11}N_3O_3S$, with molecular weight 253.279 g/mol. The systematic (IUPAC) name of sulfamethoxazole is 4-Amino-N-(5-methylisoxazol-3-yl)-benzenesulfonamide, and its molecular structure is represented in Figure (1).

*** Corresponding Author:** E. M. Attia, Chemistry Department, Faculty of Science (Girls), Al-Azhar University, Nasr City, Cairo, Egypt.

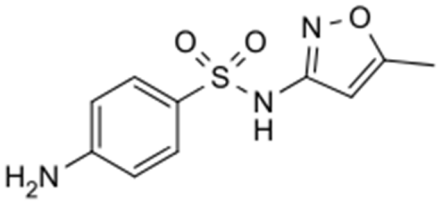

Figure 1: Molecular structure of sulfamethoxazole.

Each 5 ml of Septrin suspension contains 200 mg sulfamethoxazole and 40 mg Trimethoprim, the active ingredients of septrin syrup. The empirical formula of Trimethoprim is $C_{14}H_{18}N_4O_3$ with molecular weight 290.3g/mol, and systematic (IUPAC) name is 5-(3,4,5-Trimethoxybenzyl) pyrimidine-2,4-diamine. The molecular structure is represented in Figure (2). IR analysis was performed to determine the functional groups that still present after expiration in the two expired drugs.

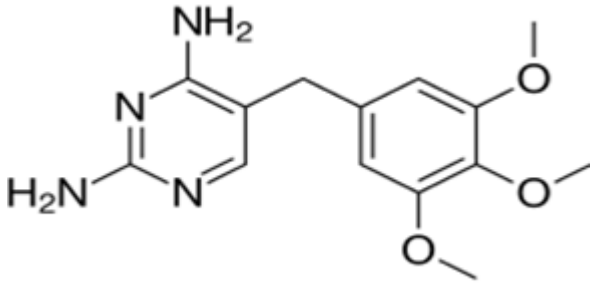

Figure 2: Molecular structure of Trimethoprim

2.2. Potentiodynamic polarization measurements:-

Potentiodynamic polarization measurements were generated using Electronic Potentioscan Wenking (Model POS 73). A platinum sheet was used as a counter electrode and a saturated calomel electrode (SCE) was used as reference electrode. The E– log I curves for all solutions were swept from -2000 mV/SCE to +2000 mV/SCE at scan rate 2 mVs^{-1}. The corrosion rate (C_R) in mpy, was calculated using Eq.1[12]:

$$C_R = 0.13 \times I_{corr} \times e/d \qquad (1)$$

where 0.13 is the metric and time conversion factor, I_{corr} is the corrosion current density in $\mu A/cm^2$, e and d are the equivalent weight and density of tin metal in geq/mol and g/cm^3 respectively. Values of I_{corr} and corrosion potential (E_{corr}) were evaluated from intersection of the linear anodic and cathodic branches of Tafel plots. Degrees of surface coverage (θ) were calculated using Eq. 2:

$$\theta = \left[1 - \frac{I_{corr}}{I^{\circ}_{corr}}\right] \qquad (2)$$

where I°_{corr} and I_{corr} are the corrosion current densities in absence and presence of inhibitors, respectively. The inhibition efficiency IE% was calculated according to Eq. 3:

$$IE\% = \theta \times 100 \qquad (3)$$

2.3. Surface characterization:-

After exposer to 1M HCl in the absence and presence of 9%(v/v) of ESD and ESpD for 2h immersion at 20°C, the surface morphologies of tin coupons were examined by scanning electron microscope (SEM).

3. RESULTS AND DISCUSSION

3.1. IR analysis:-

Figure 3-a represents the IR spectrum of ESD which illustrated very broad bands due to NH_2 and NH groups, and another broad band due to (C=O). Also, band due to $\nu_{asym}(SO_2)$ at 1050 cm^{-1} and band due to C=N at 1623 cm^{-1} were detected. In ESpD (Figure 3-b); very broad band at 1200 cm^{-1} and band due to $\nu_{sym}(SO_2)$ appeared at 1400 cm^{-1} were detected. The spectrum of ESpD also illustrated the presence of C=N at 1600 cm^{-1} and presence of aromatic C-H band. All the charts of IR spectrum were analyzed according to Stuart [19].

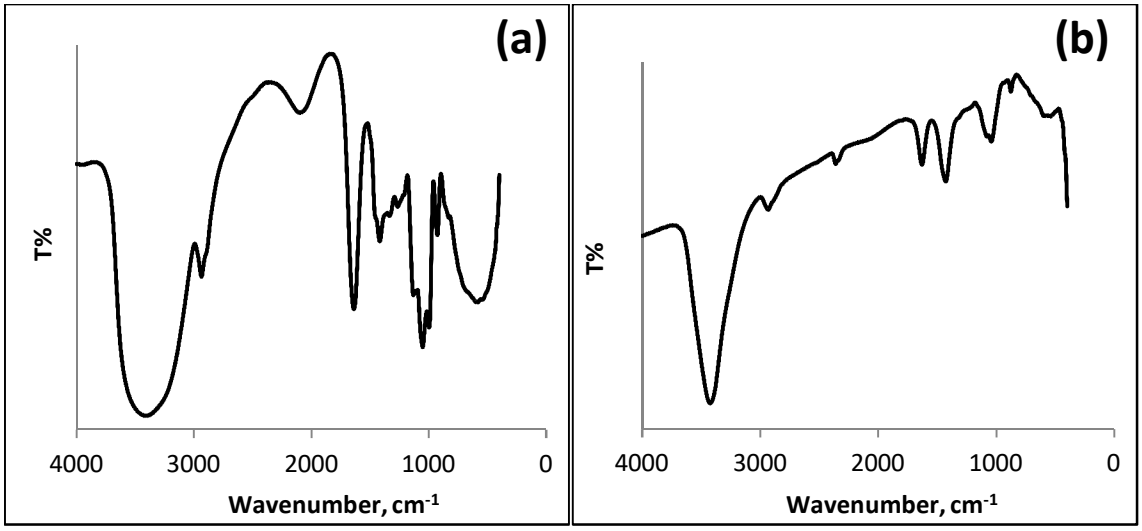

Figure 3: IR spectrum of (a) ESD and (b) ESpD.

3.2. Potentiodynamic polarization

3.2.1. Effect of solution composition

The polarization experiments (Figure 4) illustrated that, the cathodic branches of Sn electrode exhibited the highest current density (c.d.) in blank solution (0% inhibitor), and the lowest c.d. in ESpD solution. The reverse behavior was observed in the anodic branches till the potential sweep reached to 0 V/SCE. However, all the anodic branches of the Sn electrode are about to coincide in the potential range 0 – 2 V/SCE. This confirmed the higher corrosion resistance of Sn electrode under cathodic polarization conditions in ESpD solution.

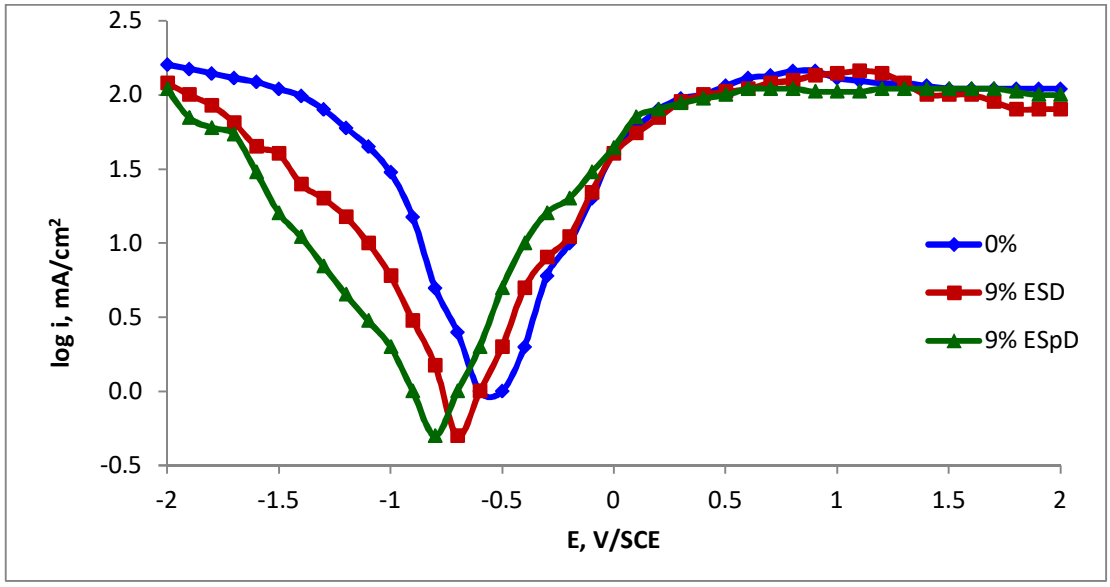

Figure 4: Potentiodynamic polarization plot of Sn electrode in 1M HCl in absence (0%) and presence of 9% of ESD and ESpD at 20°C.

3.2.2. Effect of temperature

It was observed from Figure (5) that the general shape of the polarization curves did not change with changing temperature. The respective potentiodynamic parameters including corrosion potential (E_{corr}), corrosion current density (I_{corr}), corrosion rate (C_R), anodic (β_a) and cathodic (β_c) Tafel slopes are tabulated in Table 1.

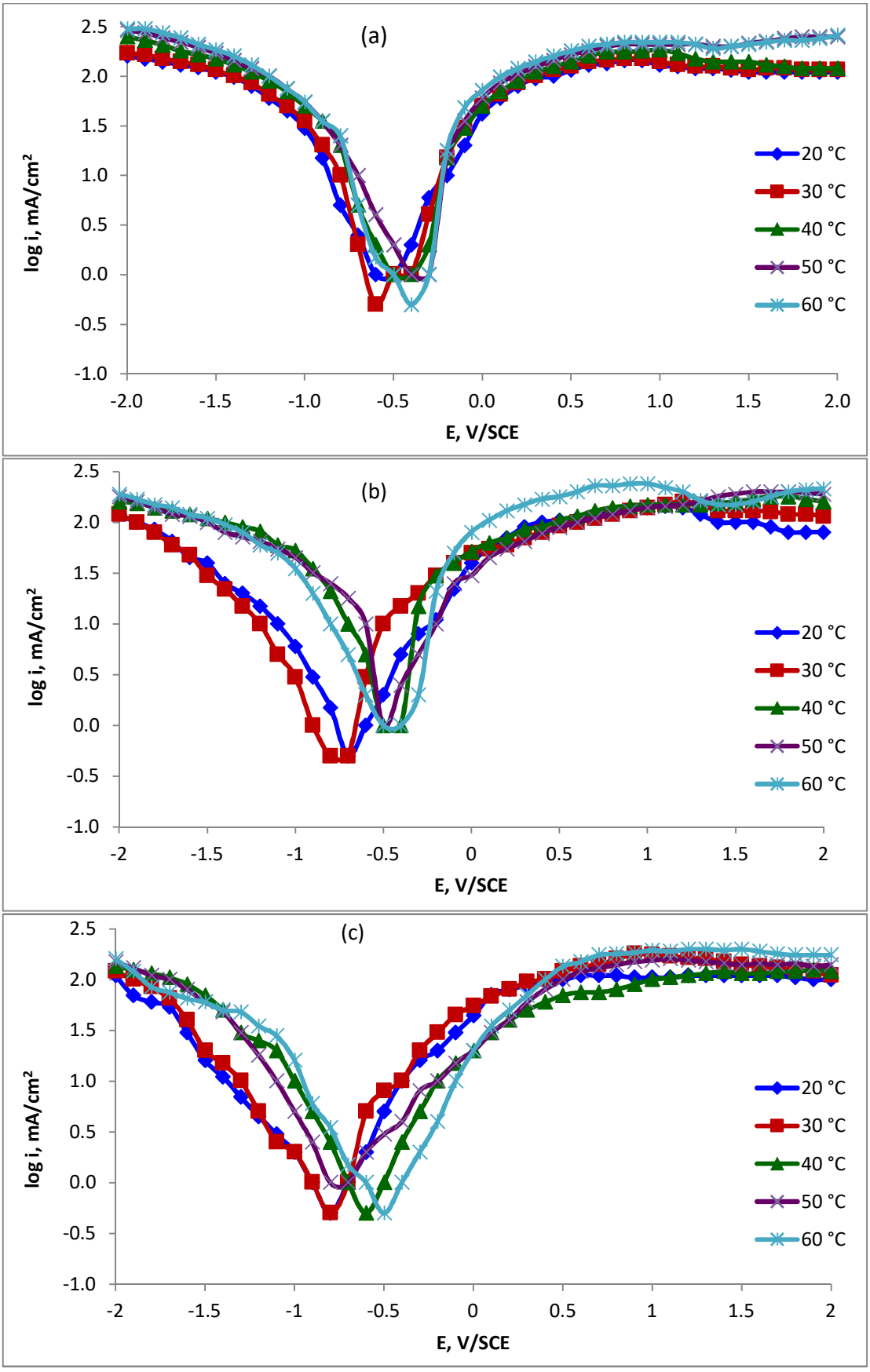

Figure 5: Potentiodynamic polarization plots of Sn electrode at different temperatures in: (a) blank HCl, (b) HCl containing 9% ESD and (c) HCl containing 9% ESpD.

Table 1: Potentiodynamic parameters for Sn electrode in absence and presence of 9 %(v/v) of ESD and ESpD at temperatures range of 20- 60°C

Expired Drug	Temp.	E_{corr}, mV/SCE	I_{corr}, mA/cm^2	βa, mV/dec	$-\beta c$ mV/dec	θ	IE%	C_R, mpy
Blank	20	-550	50.1	2000	1000	-	-	52903
	30	-600	63.1	1000	1000	-	-	66605
	40	-450	66.1	1428	666	-	-	69740
	50	-400	70.8	1666	833	-	-	74733
	60	-400	112.2	10000	1250	-	-	118433
ESD	20	-500	2.5	588	666	0.9500	95.00	2645
	30	-580	3.2	588	769	0.9498	94.98	3337
	40	-600	4.0	400	416	0.9397	93.97	4202
	50	-700	5.0	1000	500	0.9292	92.92	5290
	60	-680	10.0	769	666	0.9108	91.08	10555
ESpD	20	-600	5.0	769	1000	0.8999	89.99	5290
	30	-620	6.9	666	769	0.8900	89.00	7327
	40	-685	7.9	1428	1000	0.8797	87.97	8384
	50	-700	10.0	1666	1000	0.8587	85.87	10555
	60	-740	18.2	1428	1000	0.8377	83.77	19222

As stated in previous studies; if the displacement in E_{corr} is lower than 85mV in relation to that measured for blank solution, the inhibitor can be classified as mixed type [20]. Thus, According to Table 1; ESD and ESpD acted as mixed type inhibitors at 20 and 30°C, and acted as cathodic inhibitors at 40, 50 and 60°C. This behavior was similar to that of expired primperan drug in the same corrosive medium [13].

Table 1 illustrated that, corrosion current densities and corrosion rates increased with increasing temperature in both uninhibited and inhibited solutions. Besides, the increase of corrosion rates was more pronounced with the rising of temperature for free acid solutions. These results confirmed that expired drugs under tests acted as effective inhibitors in the studied temperature range. By increasing the temperature, ESD and ESpD, may separate to more aggressive smaller components, causing increase in the corrosion rates and decrease in the inhibition efficiencies suggesting physical adsorption on the tin surface [21].

Table (1) also illustrated that; at all studied temperatures, ESD provides lower corrosion rates and higher inhibition efficiencies than ESpD. These results are not in contrast with that obtained from Figure 4 which illustrates that, the lowest c.d. was produced in ESpD solution. That is the corrosion rate values in Table (1) were for the whole reaction involving anodic and cathodic parts while the lowest c.d. produced in ESpD solution (Figure 4) was special for cathodic reaction only.

3.2.3. Kinetic and thermodynamic corrosion parameters:-

The dependence of corrosion rate on temperature was demonstrated by Arrhenius equation which was represented in Eq. 4.

$$\log C_R = A - (E_a^*/2.303\,RT) \qquad (4)$$

where A is the extrapolation factor, E_a^* is the activation energy, R is the universal gas constant and T is the absolute temperature. Figure (6-a) showed the graphical representation of Arrhenius equation, while the calculated values of activation energies derived from the slopes of the plots were listed in Table (2).

In order to calculate the enthalpy ΔH^* and entropy ΔS^* of activation for the corrosion process, the Eyring transition state (Eq. 5) was used.

$$\log C_R/T = \log(R/Nh) + (\Delta S^*/2.303R) - (\Delta H^*/2.303RT) \qquad (5)$$

Where N is Avogadro's number and h is the Planck's constant. Figure (6-b) showed the plots of $\log C_R/T$ against $1/T$. Straight lines are obtained with a slope of $(-\Delta H^*/2.303R)$ and intercept of $[\log(R/Nh) + (\Delta S^*/2.303R)]$ from which the value of ΔH^* and ΔS^* were calculated and given in Table (2).

Figure 6 (a and b) illustrated that, as the temperature was raised, the corrosion rates increased and consequently a decrease in protection efficiency was obtained. It is noted from Table 2 that the values of E_a^* and ΔH^* were higher in the presence of ESD and ESpD than in their absence, which

confirmed higher protection efficiency. This might be attributed to increasing the height of the energy barrier for the reaction, that is, a process of adsorption led to a rise in activation energy and enthalpy of the corrosion process [8]. It was also noted from Table 2 that values of E_a^* were ~ 26 and 24 kJ/mol, for ESD and ESpD respectively, meaning that the corrosion process was controlled by surface reaction [22]. The positive values of ΔH* indicated the endothermic nature of the activation process which suggested its difficult and slow dissolution in presence of tested expired drugs. The values of ΔS^* in the absence and presence of ESD and ESpD had large and negative values. This reflects the formation of an ordered stable layer of inhibitor on the tin surface [23]

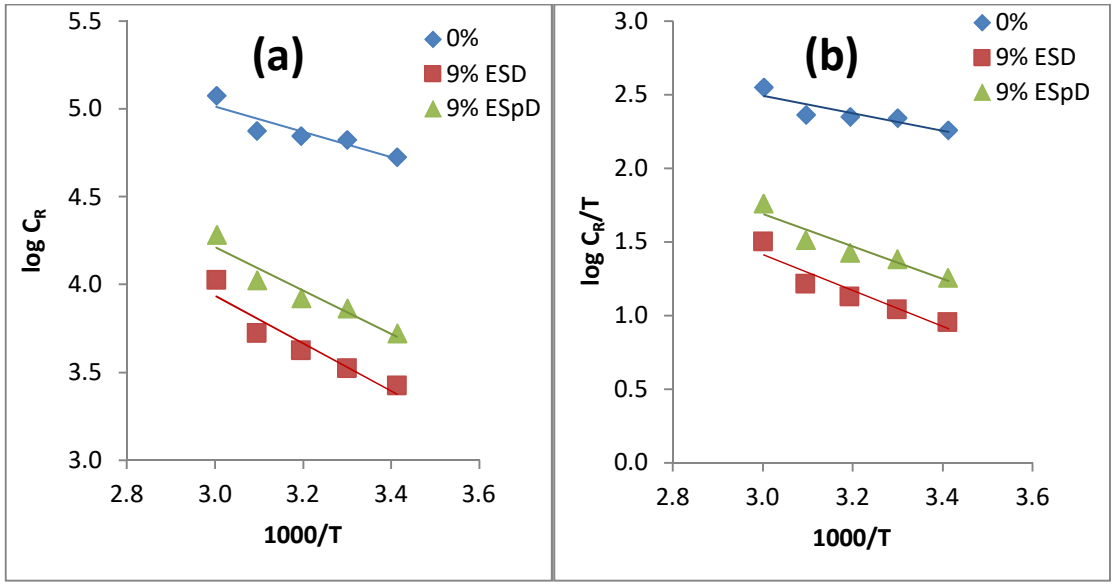

Figure 6: (a) Arrhenius and (b) Eyring transition state plots for Sn electrode in 1M HCl in absence and presence of 9% of ESD and ESpD.

Table 2: Activation parameters of Sn electrode in 1M HCl in absence and presence of 9% of ESD and ESpD

Solution	E_a^* KJ/mol	ΔH^* KJ/mol	ΔS^* J/mol.K
Blank	13.90	11.30	-173.40
ESD	25.94	23.34	-100.48
ESpD	23.72	21.12	-101.83

3.2.4. Scanning electron microscopic study (SEM):-

Figure (7-a) showed the original surface of abraded tin before contact with corrosive solution (1M HCl). It was observed that some fine scratches resulting from the grounding progress are visible in the images. Figure (7-b) showed the surface state of tin after exposure for 2h to free 1M HCl solution. Inhomogeneous layers of corrosion products were covering the surface.

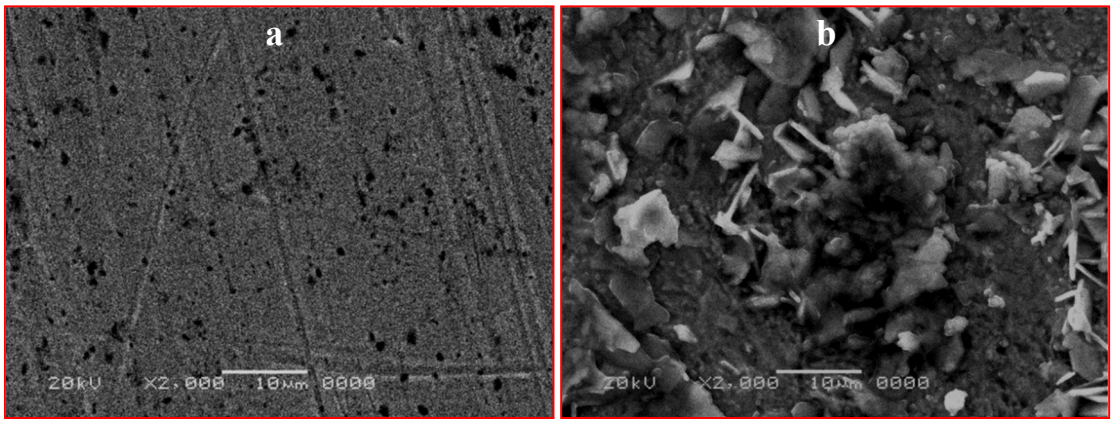

Figure 7: SEM morphology of (a) abraded Sn, (b) Sn in free HCl

In presence of 9% ESD and ESpD (Figure 8), the tin specimen had a better morphology and smoother surface when compared with the surface immersed in free 1M HCl. Intense protective layers were formed, but these layers were still less dense than that observed in expired primperan drug performed in a previous study [13]. The SEM morphology of the adsorbed protective film on the tin surface confirmed performance of inhibitive effect of ESD and ESpD.

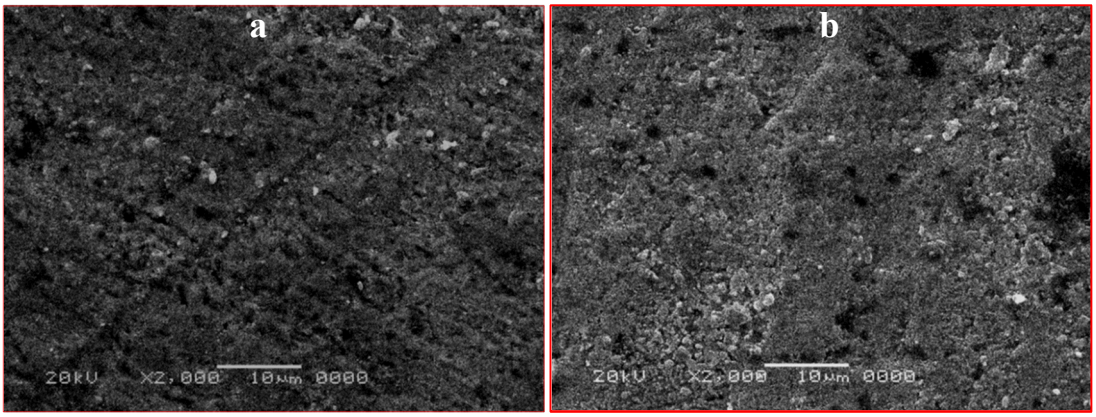

Figure 8: SEM morphology of Sn in (a) ESD, (b) ESpD

Inhibition Mechanism

The IR spectrum for ESD illustrated the presence of N–H, C=N, C=O and S=O bonds. Owing to the acidity of the medium, the tin surface acquires positive charge, and also the oxygen and sulfur atoms in the sulfamidic group could be protonated easily. This creates electrostatic repulsion between the tin surface and the protonated species. In this case, the negative chloride ions come close to the interface and facilitate the adsorption of the positively charged ESD molecules to the surface.

Septrin Drug has the same amount of the active ingredient (Sulfamethoxazole) present in Septazole in addition to trimethoprim in a ratio of 5:1, respectively. Since the molecular weight of these compounds is large (Total molecular weight for the two ingredients are 543.6 g/mol), inhibition may be effected by hindering of attacks caused by aggressive species. The cooperative action of Sulfamethoxazole and trimethoprim leads to increasing the surface coverage on the tin electrode.

According to the concept of molecular adsorption, it was expected that ESpD provides tin with better inhibition efficiency than that provided by ESD due to the presence of the two compounds of high molecular weights. Surprisingly, ESpD provides tin with the greatest C_R values at all concentrations and temperatures. This unexpected behavior may be due to higher expiration effect of ESpD. This expiration effect may lead to formation of smaller compounds with higher aggressive action. The action of the inhibitor molecules may be due to the presence of N, S, O heteroatoms as well as the aromatic ring which contain π-electrons in its molecular structure (as illustrated from IR spectrum). The decrease in inhibition efficiency with rise in temperature supports electrostatic interaction with mechanism analogous to that proposed for ESD.

CONCLUSION

1. ESD and ESpD acted as mixed type inhibitors at 20 and 30°C, and acted as cathodic inhibitors at 40, 50 and 60°C.
2. Corrosion rates increased with increasing temperature in both uninhibited and inhibited solutions, and were more pronounced for free acid solutions.
3. For the two tested expired drugs the inhibition efficiency decreased with increasing temperature, suggesting physical adsorption on the tin surface.
4. At all studied temperatures, ESD provides lower corrosion rates and higher inhibition efficiencies than ESpD.

REFERENCES

1- S.D. Kapusta and N. Hackerman; anodic passivation of tin in slightly alkaline solutions. Electrochim. Acta, 25 (1980) 1625-1639.
2- C.M.V.B. Almeida and B.F. Giannetti; Protective film growth on tin in perchlorate and citric acid electrolytes. Mat. Chem. Phys., 69 (2001) 261–266.
3- S.S. Abd El Rehim, A.M. Zaky and N.F. Mohamed; Electrochemical behaviour of a tin electrode in tartaric acid solutions. J. Allo. Comp., 424 (2006) 88–92.
4- C.A. Gervasi, P.A. Palacios, M.V. Fiori Bimbi and P.E. Alvarez; Electrochemical studies on the anodic behavior of tin in citrate buffer solutions. J. Electroanal. Chem., 639 (2010) 141–146.
5- X. Zhong, G. Zhang, Y. Qiu, Z. Chen, X. Guo and C. Fu; The corrosion of tin under thin electrolyte layers containing chloride. Corros. Sci., 66 (2013) 14–25.
6- R. M. El-Sherif and W. A. Badawy; Mechanism of Corrosion and Corrosion Inhibition of Tin in Aqueous Solutions Containing Tartaric Acid. Int. J. Electrochem. Sci., 6 (2011) 6469 – 6482.
7- N. Kumpawat, A. Chaturvedi and R. K. Upadhyay; Comparative Study of Corrosion Inhibition Efficiency of Naturally Occurring Ecofriendly Varieties of Holy Basil (Tulsi) for Tin in HNO_3 Solution. Open Journal of Metal, 2(2012) 68-73.
8- A.S. Fouda, S.A. Abdel-Maksoud and A.E. Almetwally ; Corrosion Inhibition of Tin in Sodium Chloride Solutions Using Propaneitrile Derivatives. Chem Sci Trans., 4(1)(2015)161-175.
9- S.K. Sharma, A. Peter and I.B. Obot; Potential of Azadirachta indica as a green corrosion inhibitor against mild steel, aluminum, and tin: a review. JAST 6(2015) 26.
10- O.P. Meena, A. Chaturvedi and R.B. Pareek; Comparative Study of Corrosion Inhibition Efficiency of Phyllanthus niruri for Tin in Different Solutions of HCl and H_2SO_4. (IOSR-PHR) 7(7) (2017) 40-46.
11- E.M. Attia; Expired Farcolin Drug as Corrosion Inhibitor for Carbon Steel in 1M HCl Solution. J. Basic. Appl. Chem., 5(1)(2015)1-15.
12- E.M. Attia, N.S. Hassan and A.M. Hyba; Corrosion Protection of Tin in 1M HCl by Expired Novacid Drug-Part I. Int. J. of Adv. Res. 4(2)(2016)872 –886.
13- E.M. Attia, N.S. Hassan and A.M. Hyba; Corrosion Protection of Tin in 1M HCl by Expired Primperan and E-mox Drugs-Part I. J. Basic. Appl. Chem., 7(1)(2017)9-25.
14- E.M. Attia, N.S. Hassan and A.M. Hyba; Expired Novacid Drug as a Corrosion inhibitor for Tin electrode in 1M HCl solution (open circuit potential and potentiostatic measurements)-Part II. J. Basic. Appl. Chem., 7(2)(2017)8-25.
15- P. Dohare, D.S. Chauhana and M.A. Quraishi; Expired Podocip drug as potential corrosion inhibitor for carbon steel in acid chloride solution. Int. J. Corros. Scale Inhib., 7(1)(2018) 25–37.
16- E.M. Attia, N.S. Hassan and A.M. Hyba; Corrosion Protection of Tin in 1M HCl by Expired Primperan and E-mox Drugs-Part II (weight loss study). J. Basic. Appl. Chem., 8(2)(2018)1-13.
17- A.S. Fouda, M.N. EL-Haddad and Y.M. Abdallah; Septazole: Antibacterial drug as a green corrosion inhibitor for copper in hydrochloric acid solutions. IJIRSET., 2(12)(2013)7073.
18- T. Ramdé, S. Rossi, L. Bonou; Corrosion Inhibition Action of Sulfamethoxazole for brass in acidic media. Int. J. Electrochem. Sci., 11 (2016) 6819 – 6829.
19- B. Stuart, Infrared Spectroscopy: Fundamentals and Applications, John Wiley and Sons, (2004).
20- S.H. Kumar, S. Karthikeyan, S. Narayanan and K.N. Srinivasan; Inhibition effect of Amoxycillin drug on the corrosion of mild steel in 1N hydrochloric acid solution. IJCRGG., 4(3) (2012)1077-1084.
21- A.S. Fouda and H.E. Gadow; Streptoquin and Septazole: Antibiotic drugs as corrosion inhibitors for copper in aqueous solutions. GJRE., 14(2)(2014) 22-36.
22- A.S. Fouda, F.E. Heakal, and M.S. Radwan; Role of some thiadiazole derivatives as inhibitors for the corrosion of C-steel in 1 M H_2SO_4. J. Appl. Electrochem., 39(3) (2009) 391-402.
23- A.M. Al-Bonayan; Corrosion inhibition of carbon steel in hydrochloric acid solution by Senna-Italica extract. IJRRAS., 22 (2) (2015)49-64.